

# 1 **B-cell intrinsic RANK signaling cooperates with TCL1 to induce lineage-** 2 **dependent B-cell transformation**

3

4

## 5 **SUPPLEMENTARY DATA**

6

## 7 **MATERIAL AND METHODS**

8 **Mice.** RANK<sup>K240E</sup> [1] were crossed to the E $\mu$ -TCL1-transgenic mouse model [2] to generate  
9 triple-transgenic E $\mu$ -TCL1 RANK<sup>K240E</sup> CD19<sup>Cre</sup> mice (TC-RK). For genetically deletion of  
10 CD19, we crossed our TC-RK mice to CD19<sup>Cre/Cre</sup> mice [3] to generate E $\mu$ -TCL1 RANK<sup>K240E</sup>  
11 CD19<sup>Cre/Cre</sup> (TC-RK<sup>CD19KO</sup>), E $\mu$ -TCL1 CD19<sup>Cre/Cre</sup> (TC<sup>CD19KO</sup>) and RANK<sup>K240E</sup> CD19<sup>Cre/Cre</sup>  
12 (RK<sup>CD19KO</sup>) mice. For murine MM cell transplantation, 1-2 x 10<sup>7</sup> splenocytes or 0.4-1.7 x 10<sup>6</sup>  
13 bone marrow-derived cells of diseased TC-RK mice were injected intravenously into Rag2<sup>ko</sup>  
14 mice purchased from Jackson laboratories. Mice were sacrificed upon sign of disease. For  
15 transplanting B2-cells, sorted CD19<sup>+</sup>CD5<sup>neg</sup> BM-derived cells from 4-months old TC-RK mice  
16 were transplanted into Rag2<sup>ko</sup> mice. Engraftment and B-cell stages were monitored by  
17 analysing the GFP/CD19/CD5 cell content in the peripheral blood using flow cytometry. After  
18 4 to 6 months, animals were sacrificed and spleens were analyzed for plasma cells. For the  
19 human MM Xenograft Model, we used NSG mice (*NOD.Cg-Prkdcscid Il2rgtm1Wjl/SzJ*)  
20 purchased from Janvier laboratory as recipients for the human MM cell line L363. Animals  
21 were randomly assigned to two groups and pretreated with either anti-RANKL antibody therapy  
22 (intraperitoneal, 5 mg/kg, Bio X Cell, Lebanon, US) or PBS one day before L363 injection  
23 (intravenous, 4.5 x 10<sup>6</sup> cells per mouse) and the day afterwards. Mice were sacrificed upon signs  
24 of paralysis or disease. Staff members at the Center of Preclinical Research (Technical  
25 University Munich, Munich) who were blinded to the experimental conditions and animal  
26 genotypes of the study assisted in determining when euthanasia was required. All animal  
27 experiments were conducted in accordance with German Federal Animal Protection Laws and  
28 approved by the Institutional Animal Care and use Committee at the Technical University of  
29 Munich.

30

31 **Cell culture.** The human MM cell line L363, authenticated by short tandem repeat profiling  
32 (Cell Line Authentication Service of Eurofins Genomics, Ebersberg, Germany) and murine B-  
33 cells were cultured in RPMI-Glutamax<sup>TM</sup> medium supplemented with 10 % FBS and 1%  
34 Penicillin-Streptomycin (PenStrep). Medium for naïve murine B-cells was additionally

35 supplemented with 1% nonessential amino acids, 1% sodium pyruvate, 1% HEPES and 0.05  
36 mM  $\beta$ -mercaptoethanol. RANK-expressing BAL17 cell lines [1] were cultured in RPMI  
37 Glutamax<sup>TM</sup> medium supplemented with 10 % FBS, 0.05 mM  $\beta$ -mercaptoethanol and 1%  
38 PenStrep. All cells were cultured under standard conditions; at 37 °C, 5% CO<sub>2</sub> and 95%  
39 humidity and cell lines were regularly tested for mycoplasma by PCR.

40

41 **Cell purification and stimulation.** For murine *in vitro* differentiation, naïve splenic B-cells  
42 were purified using the murine B-cell isolation kit from Miltenyi Biotec. To increase the purity  
43 of untouched B-cells, Biotin conjugated antibodies against CD5 (Clone 53-7.3, BioLegend<sup>®</sup>)  
44 and CD138 (Clone 281-2, BioLegend<sup>®</sup>) were added to the Biotin-Antibody Cocktail of the kit.  
45 2x10<sup>5</sup> B-cells were seeded per 96 flat-bottom well and stimulated either with a combination of  
46 LPS (1  $\mu$ g/mL, Sigma) and recombinant murine IL4 (1 ng/mL, PeproTech, Cranbury, US),  
47 LPS<sup>low</sup> (100 ng/mL, Sigma) in absence or presence of recombinant murine RANKL (50 ng/mL,  
48 #462-TR-010, R&D Systems, Minneapolis, US), anti-IgM (5  $\mu$ g/mL, Jackson Immuno  
49 Research) or anti-CD40 (5  $\mu$ g/mL, clone FGK45, Biolegend) in technical triplicates. RANK-  
50 expressing BAL17 cell lines were stimulated for 5 minutes with either recombinant murine  
51 RANKL (50 ng/mL) and/or anti-IgM (5  $\mu$ g/mL, Jackson Immuno Research) and afterwards  
52 directly harvested for Immunoblotting.

53

54 **Immunoblotting.** Whole cell lysates were generated by using RIPA lysis buffer supplemented  
55 with protease and phosphatase inhibitors (cOmplete<sup>TM</sup> EDTA-free protease inhibitor cocktail,  
56 Roche phosphatase inhibitor cocktail) and protein concentrations were determined by Pierce  
57 BCA Protein Assay Kit (Thermo Fisher Scientific). 15  $\mu$ g of protein was used for SDS page  
58 and transferred onto nitrocellulose membrane. Membranes were blocked for 1 h in 5 % BSA in  
59 tris-buffered saline with Tween 20 (TBST, 0.1 % Tween 20) and probed with the following  
60 primary and secondary antibodies: anti- $\beta$  actin (#60008-I-Ig, Proteintech), anti-AKT (#9272,  
61 Cell Signaling), anti-ERK (#9102, Cell Signaling), anti-pAKT (#4056, Cell Signaling), anti-  
62 pERK (#4370, Cell Signaling), anti-pJNK (#9251, Cell Signaling), anti-JNK (#sc-7345, Santa  
63 Cruz), anti-RANK (#sc-374360, Santa Cruz), anti-pSRC family (#2101, Cell Signaling), anti-  
64 SRC (2110, Cell Signaling), anti-pPLC $\gamma$ 2 (#3871, Cell Signaling), anti-PLC $\gamma$ 2 (#3872, Cell  
65 Signaling), anti-pIkk $\alpha/\beta$  (#2078, Cell Signaling), anti-Ikk $\alpha$  (#2682, Cell Signaling) and anti- $\alpha$   
66 tubulin (#12351, Cell signaling), anti-rabbit IgG-HRP (#7074 Cell Signaling) and anti-mouse  
67 IgG (#7076, Cell Signaling). Blots were imaged on a ChemiDoc MP Imaging System (Bio-

68 Rad, Hercules, US). Densitometry quantification was acquired using the Licor Image Studio  
69 Lite software.

70 **RBC count.** Blood samples were collected in EDTA blood collection tubes and RBC count  
71 was measured using scil Vet abc Plus+ device (scil animal care company GmbH, Viernheim,  
72 Germany) according to the manufacturer's protocol.

73 **Measurement of plasma proteins and immunoglobulins.** Serum electrophoresis was  
74 conducted in the routine laboratory of the Institute of Clinical Chemistry and Pathobiology at  
75 the Klinikum rechts der Isar, Munich. Detection of immunoglobulin and proteins were  
76 performed using the LEGENDplex™ Mouse Immunoglobulin Isotyping Panel and Mouse B-  
77 cell Panel Standard manufactured by BioLegend® (San Diego, US) according to the  
78 manufacturer's instructions.

79

80 **Flow cytometry.** Peripheral blood and organs were harvested from mice and single cell  
81 suspensions were processed as previously described [1]. Flow Cytometry data was acquired  
82 using a FACS Canto II cytometer and analyzed with the FlowJo™ software version 10.8.1 (BD  
83 Bioscience, San Diego, US). Dead cell exclusion was obtained either by using the Zombie  
84 Aqua™ Fixable Viability Kit (BioLegend®, San Diego, US) or DAPI (1 µg/ml) (Sigma Aldrich,  
85 St. Louis, US) staining. For blocking free Fc receptors, anti-mouse CD16/32 or human Fc  
86 Receptor blocking solution (BioLegend®) were applied and cells were stained with  
87 fluorochrome-labeled antibodies according to manufacturer's information. Antibodies from  
88 BioLegend® included anti-CD19-APC-Cy7 (clone 5D3, #115530), anti-CD5-PE (clone 53-7.3,  
89 #100607), anti-Blimp1-AlexaFluor674 (clone 5E7, #150003), anti-CD138-PE (clone 281-2,  
90 #142504), anti-CD138-PerCy5.5 (clone 281-2, #142510), anti-CD45R-APC-Cy7 (RA3-6B2,  
91 #103224), anti-CD23-PE-Cy7 (B3B4, #101614), anti-CD25-PE (PC61.5, #102008), anti-  
92 CD19-APC (6D5, #115512). Anti-CD21-PE (7G6, #552957) was purchased from BD  
93 Bioscience (Franklin Lakes, US). Antibodies from eBioscience (San Diego, US) included anti-  
94 CD265-PE (clone R12-31, #12-6612-82), anti-IRF4-PerCP-eFluor700 (clone 3E4, #46-9858-  
95 82), anti-IgM-PE-Cy7 (clone II/41, #25-5790-81), anti-IgD-APC (clone 11-26c (11-26), #17-  
96 5993-80), anti-CD45R-eFluor450 (RA3-6B2, #48-0452-82), anti-CD5-APC (53-7.3, #17-  
97 0051-82), anti-CD117-APC (2B8, #17-1171-81). Anti-CD265-PE (9A725, #MA1-41015) was  
98 purchased from Invitrogen (Waltham, US). Intracellular stainings were performed using the  
99 intracellular fixation & permeabilization buffer set from eBioscience.

100 **Histology.** Murine organs were fixed in 10% neutral buffered formalin for 48 hours, paraffin  
101 embedded and sectioned according to routine methods. Bones were additionally decalcified in  
102 Osteosoft® (Sigma Aldrich, St. Louis, US) for 1 week after fixation. Sections were stained with  
103 Hematoxylin-Eosin, anti-murine CD138 antibody (clone 281-2, BD Bioscience) IRF4 (M-17,  
104 Santa Cruz, Santa Cruz, US). Human MM biopsies were stained with anti-human  
105 TNFRSF11A/RANK antibody (clone 9A725, LSBio, Lynnwood, US). Slides were scanned  
106 with a Leica AT2 biosystem and both HE and IHC were analyzed and evaluated by a blinded  
107 board-certified pathologist.

108 **RNA sequencing and differential gene expression analysis.** RNA of purified plasma cells  
109 (CD138 MicroBeads, Miltenyi Biotech, Bergisch Gladbach, Germany) from RK and TC-RK  
110 mice was isolated by using a Qiagen RNeasy Mini Kit (Venlo, Netherlands) according to  
111 manufacturer's protocol. Quality control, mRNA library preparation and paired-end sequencing  
112 were subsequently performed by Novogene (Cambridge, UK) on a NovaSeq 6000 System  
113 (Illumina, San Diego, US) with a sequencing depth of 30 M reads/sample. The reference  
114 genome GRCm38.p6 was used for alignment. Differential expression analysis was performed  
115 in R (v4.2.1) with DESeq2 (v1.36) using the LRT test. A gene was considered differentially  
116 expressed if its FDR adjusted p-value was below 0.05. Gene Set enrichment analysis was  
117 performed with R (v4.2.1) using the GSEA package (v4.3.2). Analysis of gene list similarities  
118 was performed by using 'GeneOverlap' package in R (v4.3.2) [4] and Fisher's exact test was  
119 applied to determine the statistical significance.

120

121 **Single-cell RNA sequencing and analysis.** scRNA-seq was performed on BM flushes after  
122 RBC lysis pooled from 5-months-old TC-RK (n=4) compared to RK (n=3) mice. Pooled cell  
123 suspensions (one RK and one TC-RK) were immediately processed using the 10X Genomics  
124 (CA, USA) scRNA kit, following the manufacturer's instructions. Library preparation was  
125 performed according to the Chromium Single Cell 3' Reagent Kit v3.1 (10X Genomics, PN-  
126 1000269) and the 3' Feature Barcode Kit (10X Genomics, PN-1000262) according to the  
127 manufacturer's instructions. Sequencing was conducted using an Illumina NovaSeq 6000  
128 Sequencing system at the Helmholtz Munich. Subsequently, the sequencing files were  
129 processed in accordance with the 10x Genomics workflow by the Helmholtz Core Facility.  
130 Doublets were removed using the python package Scrublet [5]. Further downstream processing  
131 was performed using Seurat (v4.3.0) [6]. Quality control filtering was performed to eliminate  
132 low-quality cells with the following parameters: cells with fewer than 200 detected genes or  $\geq$   
133 10% mitochondrial reads were removed. The remaining high-quality cells were kept for

134 downstream processing. Data were normalized using the *SCTransform* function, regressing out  
135 technical confounding factors (mitochondrial reads) using the *vars.to.regress* arguments.  
136 Principal component analysis (PCA) and uniform manifold approximation and projection  
137 dimensionality reduction (UMAP) was performed based on the normalized data.  
138 Celltype annotation was performed using SingleR [7] with mouse bulk expression data from  
139 the Immunologic Genome Project (ImmGen) dataset [8] as a reference. Cell types with a low  
140 abundance (<10 cells) were eliminated, which resulted in removal of stromal cells, fibroblasts,  
141 epithelial cells, eosinophils and endothelial cells. Plasma cells were defined B-cells expressing  
142 plasma cell marker genes *Sdc1* and *Slamf7* as follows: `Plasma <- subset(x = seurat, subset =`  
143 `Sdc1 > 0.5 & Slamf7 > 0.5, idents = "B-cells")`.  
144 Marker genes for each of the conditions were identified using the *FindMarker* function from  
145 the Seurat package. The gene signatures employed in this study were obtained from the  
146 Molecular Signature Database (<https://www.gsea-msigdb.org/gsea/index.jsp>) or defined based  
147 on the literature. To characterize cell states, we computed signature scores by averaging the  
148 relative expression of gene sets. Gene-set enrichment analysis was conducted using Fgsea [9],  
149 and P values were determined by one-tailed permutation test. The Milo [10] implementation in  
150 Python (milopy package) was used to estimate changes in cell type abundance between  
151 conditions. Neighborhoods were annotated based on the predominant cell type and those  
152 neighborhoods where less than 50% of cells belonged to one cell type were labelled as "Mixed".  
153 Shown are neighborhoods with FDR<0.1.

154

155 **Whole exome sequencing and analysis.** DNA of MACS purified splenocytes using the CD138  
156 plasma cell kit (Miltenyi Biotech) from diseased TC-RK mice (n=7) was isolated by using the  
157 DNeasy® Blood & Tissue Kit (Qiagen). Quality control, mRNA library preparation and  
158 sequencing were carried out by Novogene. The sequencing was conducted on a NovaSeq  
159 System, utilizing a paired-end 150bp read format with a S4 flow cell.

160 Analysis was conducted following GATK best practice suggestions based on the established  
161 analysis pipeline MoCaSeq [11]. In brief, Trimmomatic (v0.39) was used to trim raw  
162 sequencing reads before mapping. Reads were aligned using BWA-MEM 0.7.17 with default  
163 settings and the reference genome GRCm38.p6. PCR duplicates were identified with samblaster  
164 (v0.1.26) and sambamba (v0.7.0), together with Picard tools (v2.20.0) and realignment around  
165 indels was performed using the GATK toolkit (v4.2.0.0). Somatic mutations were called by  
166 using Mutect2 with default settings, based on the paired case and control sample. Potential  
167 somatic events were filtered for SNPs by excluding single nucleotide variants (SNV) which

168 were reported in the Mouse Genome Project SNP database (v5). Furthermore,  
169 ‘LearnReadOrientationModel’ was used for exclusion of SNVs marked as strand or PCR bias  
170 artefact and annotation of somatic events was performed with SNPeff (version 4.3). SNVs with  
171 a low predicted impact and variants at non-exonic sites were excluded from further analysis.  
172 Data was deposited to ENA PRJEB73315. A comparative analysis investigated MM mutation  
173 profiles between the mouse model and the human myeloma dataset. The mutation profile of  
174 205 samples was employed from previously conducted study in 2014 [12]. This dataset was  
175 sourced from cBioPortal.

176 Copyratios were defined using CNVKit (v0.9.9). Calling was conducted using the “batch”  
177 command of the CNVKit pipeline including read coverage estimation in target and antitarget  
178 regions, normalization and segmentation. The probe regions of the whole-exome sequencing  
179 kit served as on-target regions.

180

181 **Statistical Analysis.** Statistical analyses were performed using GraphPad Prism Version 8.0,  
182 GraphPad Software Inc. Statistical significance between two groups was analyzed with paired  
183 or unpaired two-tailed Student’s t test, while ordinary one-way ANOVA with Turkey’s multiple  
184 comparison test was used for more than two groups. Kaplan-Meier plot was used for probability  
185 of survival and Log-Rank (Mantel Cox) testing was used for comparison of cohorts. Moreover,  
186 statistical methods were not used to determine the sample size in advance. All data are presented  
187 as mean  $\pm$  standard deviation.  $P < 0.05$  was considered as statistically significant.

188

189

## 190 SUPPLEMENTARY REFERENCES

191

- 192 1. Alankus, B., V. Ecker, N. Vahl, M. Braun, W. Weichert, S. Macher-Goppinger, T.  
193 Gehring, et al., *Pathological RANK signaling in B cells drives autoimmunity and*  
194 *chronic lymphocytic leukemia*. J Exp Med, 2021. **218**(2).
- 195 2. Bichi, R., S.A. Shinton, E.S. Martin, A. Koval, G.A. Calin, R. Cesari, G. Russo, et al.,  
196 *Human chronic lymphocytic leukemia modeled in mouse by targeted TCL1 expression*.  
197 Proc Natl Acad Sci U S A, 2002. **99**(10): p. 6955-60.
- 198 3. Rickert, R.C., J. Roes, and K. Rajewsky, *B lymphocyte-specific, Cre-mediated*  
199 *mutagenesis in mice*. Nucleic Acids Res, 1997. **25**(6): p. 1317-8.
- 200 4. Shen, L.J.R.P., *GeneOverlap: an R package to test and visualize gene overlaps*. 2014.
- 201 5. Wolock, S.L., R. Lopez, and A.M. Klein, *Scrublet: Computational Identification of*  
202 *Cell Doublets in Single-Cell Transcriptomic Data*. Cell Syst, 2019. **8**(4): p. 281-291  
203 e9.
- 204 6. Hao, Y., S. Hao, E. Andersen-Nissen, W.M. Mauck, 3rd, S. Zheng, A. Butler, M.J. Lee,  
205 et al., *Integrated analysis of multimodal single-cell data*. Cell, 2021. **184**(13): p. 3573-  
206 3587 e29.

- 207 7. Aran, D., A.P. Looney, L. Liu, E. Wu, V. Fong, A. Hsu, S. Chak, et al., *Reference-*  
208 *based analysis of lung single-cell sequencing reveals a transitional profibrotic*  
209 *macrophage*. Nat Immunol, 2019. **20**(2): p. 163-172.
- 210 8. Heng, T.S., M.W. Painter, and C. Immunological Genome Project, *The Immunological*  
211 *Genome Project: networks of gene expression in immune cells*. Nat Immunol, 2008.  
212 **9**(10): p. 1091-4.
- 213 9. Korotkevich G, S.V., Sergushichev A (2019). "Fast gene set enrichment analysis."  
214 bioRxiv. doi:10.1101/060012, <http://biorxiv.org/content/early/2016/06/20/060012>.
- 215 10. Dann, E., N.C. Henderson, S.A. Teichmann, M.D. Morgan, and J.C. Marioni,  
216 *Differential abundance testing on single-cell data using k-nearest neighbor graphs*.  
217 Nat Biotechnol, 2022. **40**(2): p. 245-253.
- 218 11. Lange, S., T. Engleitner, S. Mueller, R. Maresch, M. Zwiebel, L. Gonzalez-Silva, G.  
219 Schneider, et al., *Analysis pipelines for cancer genome sequencing in mice*. Nat  
220 Protoc, 2020. **15**(2): p. 266-315.
- 221 12. Lohr, J.G., P. Stojanov, S.L. Carter, P. Cruz-Gordillo, M.S. Lawrence, D. Auclair, C.  
222 Sougnez, et al., *Widespread genetic heterogeneity in multiple myeloma: implications*  
223 *for targeted therapy*. Cancer Cell, 2014. **25**(1): p. 91-101.
- 224 13. Larrayoz, M., M.J. Garcia-Barchino, J. Celay, A. Etxebeste, M. Jimenez, C. Perez, R.  
225 Ordonez, et al., *Preclinical models for prediction of immunotherapy outcomes and*  
226 *immune evasion mechanisms in genetically heterogeneous multiple myeloma*. Nat  
227 Med, 2023. **29**(3): p. 632-645.
- 228
- 229

229

## 230 SUPPLEMENTARY FIGURE LEGENDS

231

### 232 Supplementary Figure 1: Characterization of TC-RK mice and their myeloma cells

233 **a)** Dot plot graph depicts spleen (SP) size in centimeters (cm) of diseased or aged mice with  
234 indicated genotypes (n=3-9 per genotype). **b)** Dot plot graph depicts liver (LI) weight in gram  
235 (g) of diseased or aged mice with indicated genotypes (n=3-8). **c)** Geometric mean (geo. mean)  
236 of forward scatter area (FSC-A), surface RANK, CD138, B220, IgM and IgD, as well as  
237 intracellular IRF4 and BLIMP1 from GFP<sup>hi</sup>CD19<sup>neg</sup> cells (green) compared to GFP<sup>+</sup>CD19<sup>+</sup>  
238 cells (black) from TC-RK mice (n=4-5). **d)** Representative images of H&E and  
239 immunohistochemistry (CD138, IRF4) of spleens of diseased TC-RK and control mice (scale  
240 bars: overview=1mm, detailed images: 40x magnification). **e)** Kaplan-Meier OS analysis of  
241 Rag2<sup>ko</sup> mice (n=3) transplanted with TC-RK bone marrow cells derived from two different sick  
242 donor mice compared to Rag2<sup>ko</sup> control mice. **f)** Percentages of GFP<sup>hi</sup>CD19<sup>neg</sup> cells and  
243 GFP<sup>+</sup>CD19<sup>+</sup> cells of viable cells from bone marrow (BM), spleen (SP), peripheral blood (PB)  
244 and liver (LI) isolated from diseased Rag2<sup>ko</sup> mice (n=3) transplanted with TC-RK bone marrow  
245 cells derived from two different donor mice. Statistical analysis was performed using the one-  
246 way ANOVA with Tukey correction for multiple comparison and Student's t-test. P values are  
247 indicated in respective graphs. All data are presented as mean ± standard deviation.

248 **Supplementary Figure 2: *In vivo* and *in vitro* differentiation capacity of B-cells from TC-**  
249 **RK mice**

250 **a)** Bone marrow B-cell developmental stages of six-weeks-old TC-RK (n=5) and control mice  
251 (n=5-6 per genotype) were assessed by flow cytometry as follows: B220<sup>+</sup>CD19<sup>+</sup> (of living  
252 cells), IgM<sup>neg</sup> (B220<sup>+</sup>CD19<sup>+</sup>), pre B (CD25<sup>+</sup> cKit<sup>neg</sup>, IgM<sup>neg</sup>, B220<sup>+</sup>CD19<sup>+</sup>), pro B-cells  
253 (cKit<sup>+</sup>CD25<sup>neg</sup>, IgM<sup>neg</sup>, B220<sup>+</sup>CD19<sup>+</sup>), immature (IgM<sup>+</sup>B220<sup>+</sup>CD19<sup>+</sup>) recirculating  
254 (IgM<sup>+</sup>B220<sup>high</sup>, CD19<sup>+</sup>). Pooled data from three individual experiments. **b)** Percentage of  
255 splenic CD19<sup>+</sup>CD5<sup>+</sup> of viable cells pre-gated on CD19<sup>+</sup>CD5<sup>neg</sup> (right) from 6-weeks-old TC-  
256 RK (n=6) and control mice (n=4-6 per genotype). Pooled data from three individual  
257 experiments. **c)** Percentages of splenic CD21<sup>+</sup>CD23<sup>neg</sup> marginal zone (MZ) B-cells pre-gated on  
258 CD19<sup>+</sup>CD5<sup>neg</sup> (right) from six-weeks-old TC-RK (n=6) and control mice (n=4-6). Pooled data  
259 from three individual experiments. **d)** Quantification of IgA immunoglobulin isotype in  
260 supernatants from *in vitro* differentiated naïve B-cells, derived from animals with indicated  
261 genotype (n=3-5) and stimulated for four days with LPS<sup>low</sup>, by flow cytometry-based multiplex  
262 immunoassay. Pooled data from two different experiments. **e)** Experimental set up of *in vitro*  
263 differentiation of MACS-isolated naïve B-cells using a combination of LPS (1 µg/mL) and 1  
264 ng/mL recombinant murine IL4 or anti-IgM (5 µg/mL) or anti-CD40 (5 µg/mL). B-cell stages  
265 were analyzed by flow cytometry four days after stimulation. Graphic was created  
266 BioRender.com. **f)** Percentages of CD138<sup>+</sup>B220<sup>low</sup> plasma cells of living cells after *in vitro*  
267 differentiation with LPS and IL4 determined by flow cytometry four days after stimulation.  
268 Biological replicates were pooled from two individual experiments. **g)** Percentages of  
269 CD138<sup>+</sup>B220<sup>low</sup> plasma cells of living cells after *in vitro* stimulation with anti-IgM determined  
270 by flow cytometry after four days. Biological replicates were pooled from two individual  
271 experiments. **h)** Percentages of CD138<sup>+</sup>B220<sup>low</sup> plasma cells of living cells after four days *in*  
272 *vitro* stimulation with anti-CD40 determined by flow cytometry. Biological replicates were  
273 pooled from two individual experiments. Statistical analysis was performed using the one-way  
274 ANOVA with Tukey correction for multiple comparison. P values and not significant (ns)  
275 results are indicated in respective graphs. All data are presented as mean ± standard deviation.

276

277 **Supplementary Figure 3: Signaling transduction after RANK and/or BCR stimulation in**  
278 **RANK-overexpressing BAL17 B-cell lymphoma cells**

279 **a)** BAL17 pMIG, BAL17 RANK<sup>wt</sup> and BAL17 RANK<sup>K240E</sup> cells were stimulated with either  
280 murine RANKL (50 ng/mL) and/or aIgM (5 µg/mL) for 5 minutes. Representative immunoblots



281 blotted for the indicated phospho- and total proteins and a loading control from one out of three  
282 independent experiments. **b)** Densitometry quantification of phosphoproteins to their total  
283 counterparts shown in a) and normalized to the unstimulated control (-RANKL/-aIgM) from  
284 three independent experiments. Student's t-test was applied on indicated conditions to highlight  
285 effects of RANKL stimulation in RANK<sup>wt</sup>- and RANK<sup>K240E</sup>-overexpressing BAL17 cell lines.  
286

287 **Supplementary Figure 4: T and B-cell immunophenotyping within the bone marrow niche**  
288 **of TC-RK mice**

289 **a)** UMAP plots of unsupervised clustering analysis of B-cells and plasma cells (defined by *Sdc1*  
290 and *Slamf7* expression). Cells of individual UMAP plots are color coded according to *Ptprc*,  
291 *Pax5*, *Ebfl*, *Sqstm1*, *CD74*, and *Mzb1* gene expression respectively. **b)** TC-RK cells within the  
292 B and plasma cell subcluster show a higher plasma cell score. **c)** TC-RK cells with in the T cell  
293 subcluster show a higher CD8 exhaustion (Tex, left) and activation phenotype (right) as  
294 compared to RK-derived bone marrow cells.

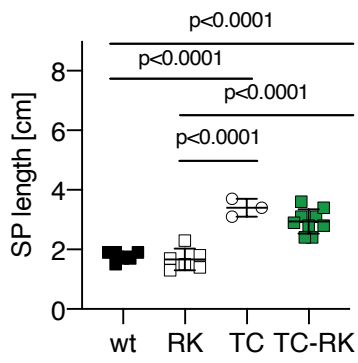
295

296 **Supplementary Figure 5: Overlap between TC-RK-induced myeloma and other murine-**  
297 **induced and human Multiple Myeloma**

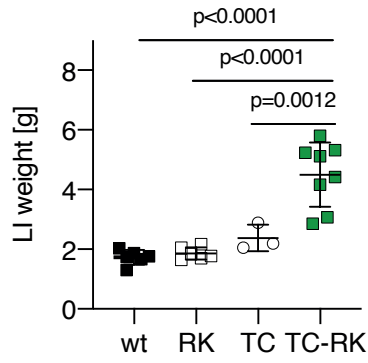
298 **a)** Table depicts differential gene expression similarities analysis including p values and odds  
299 ratios between myeloma cells from TC-RK mice compared to myeloma cells from various  
300 multiple myeloma mouse models [13]. Fisher's exact test was applied and both p values and  
301 odd ratios are depicted. **b)** Table of histological evaluation by a certified pathologist of RANK  
302 expression in human MM patients according to their percentage of myeloma cell infiltration,  
303 percentage of RANK<sup>+</sup> stained myeloma cells and staining intensity.

# Suppl. Figure 1

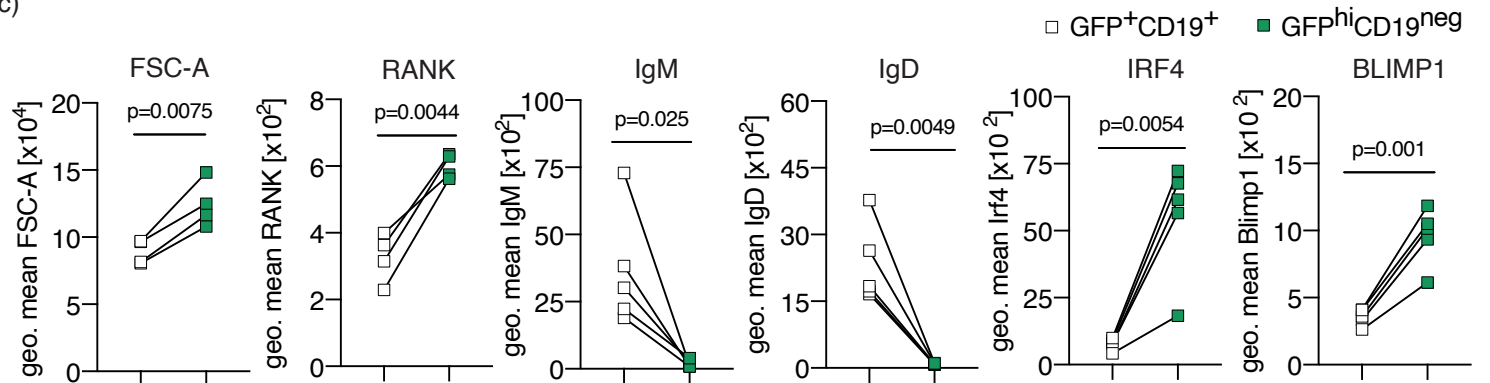
a)



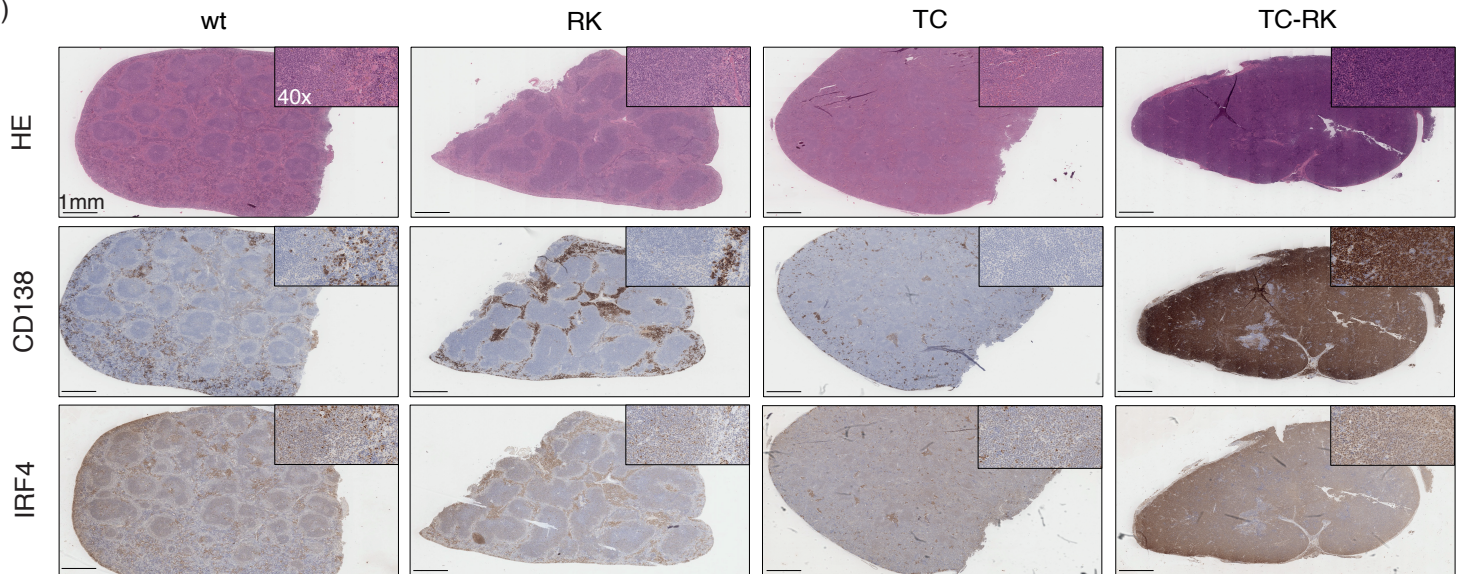
b)



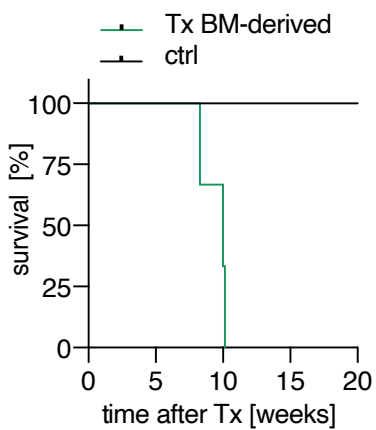
c)



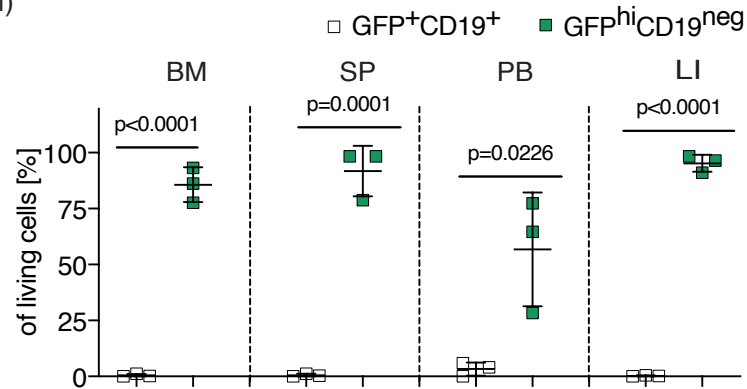
d)



e)

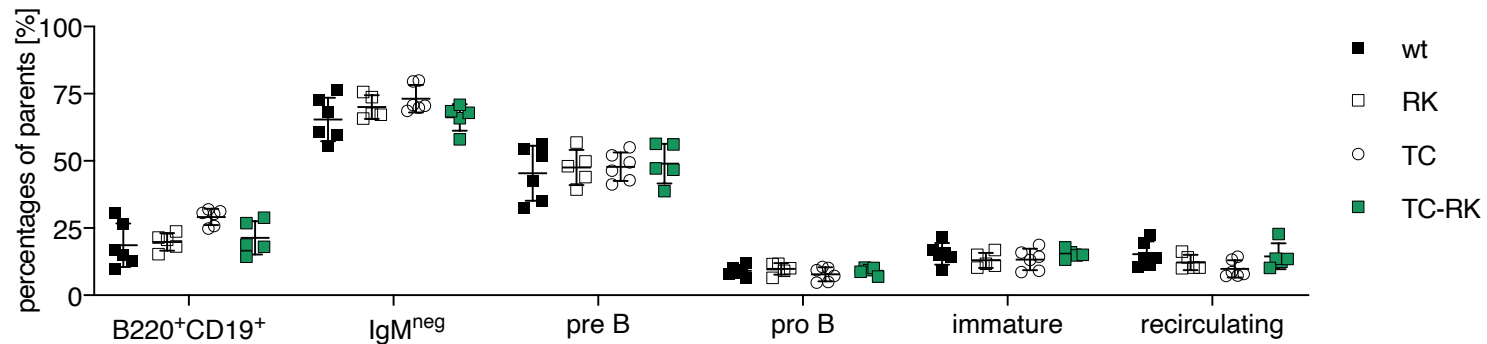


f)

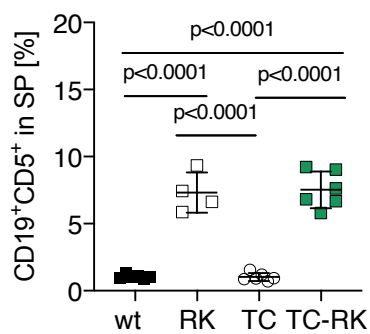


# Suppl. Figure 2

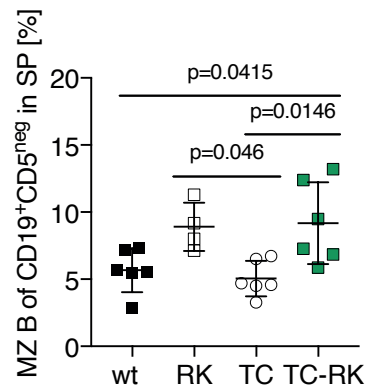
a)



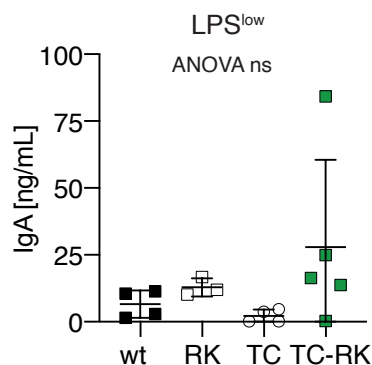
b)



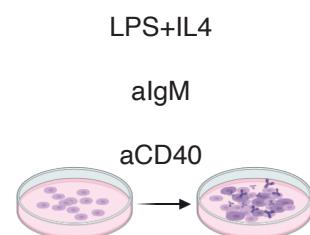
c)



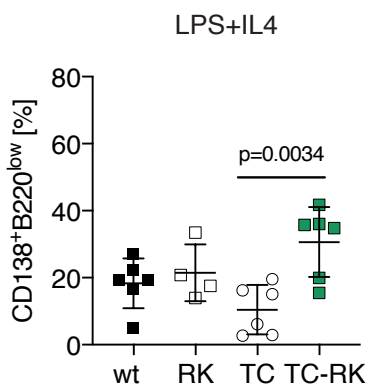
d)



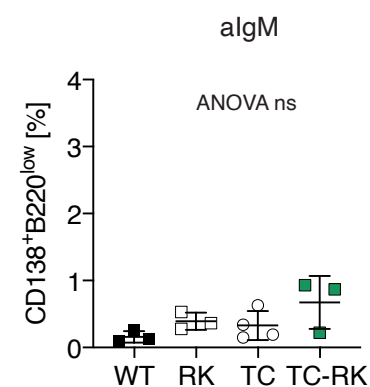
e)



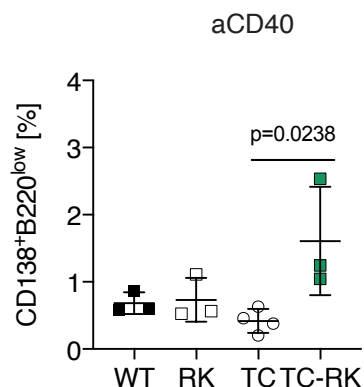
f)



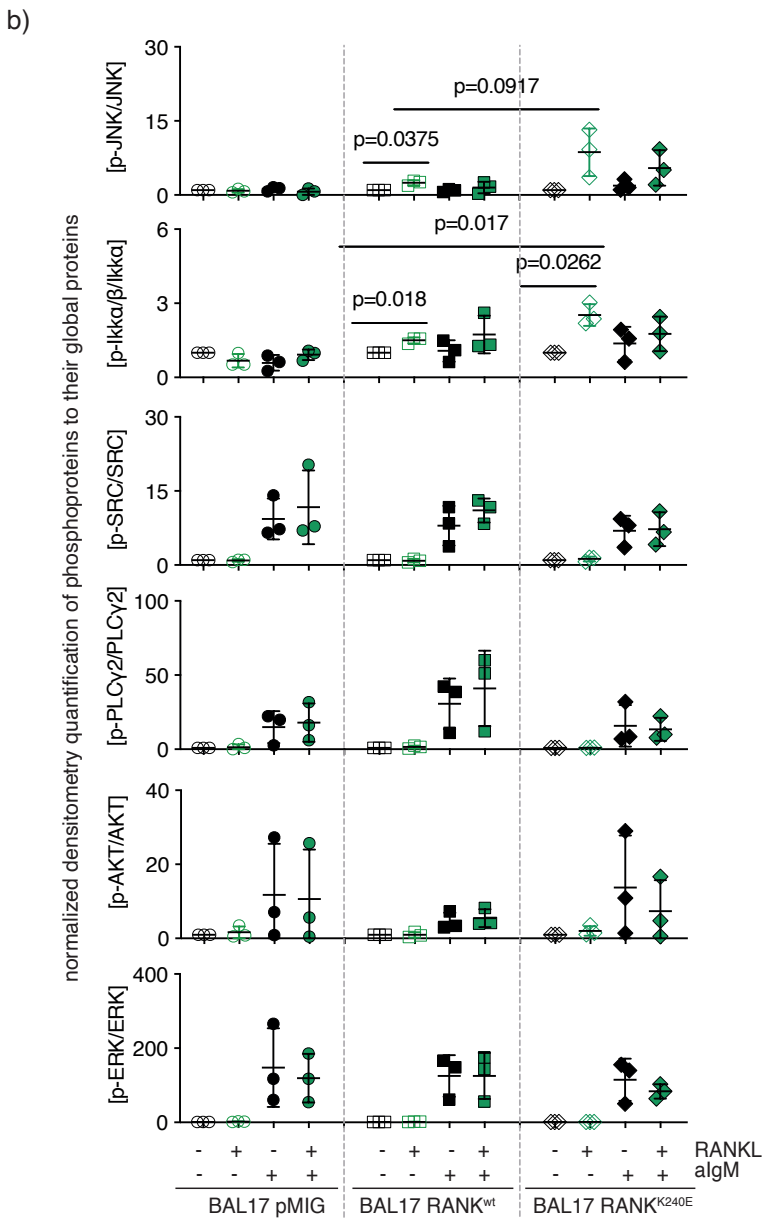
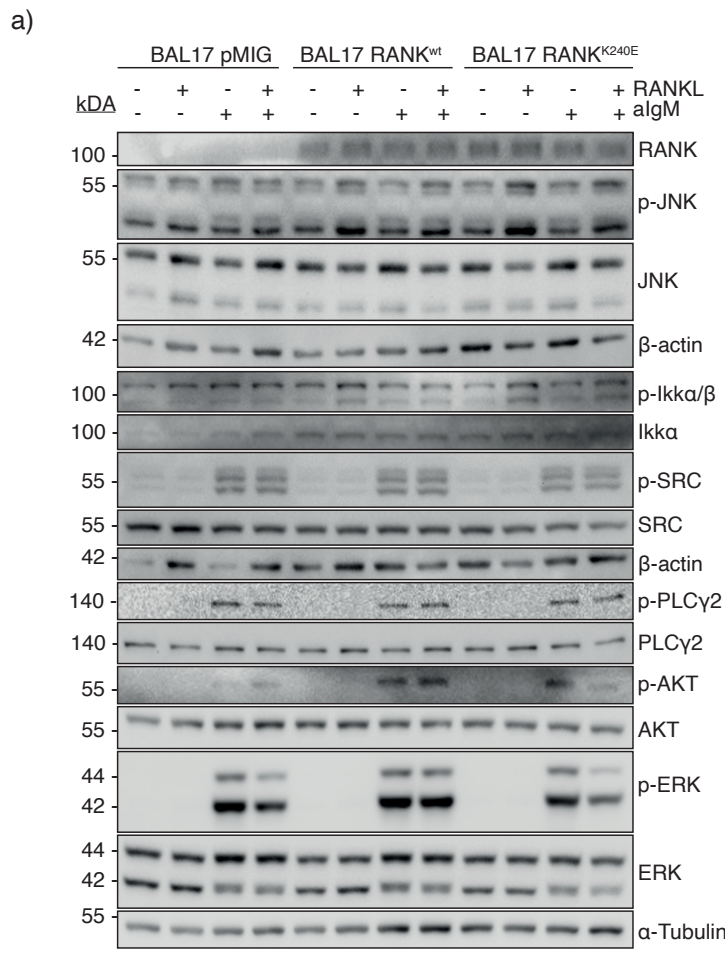
g)



h)

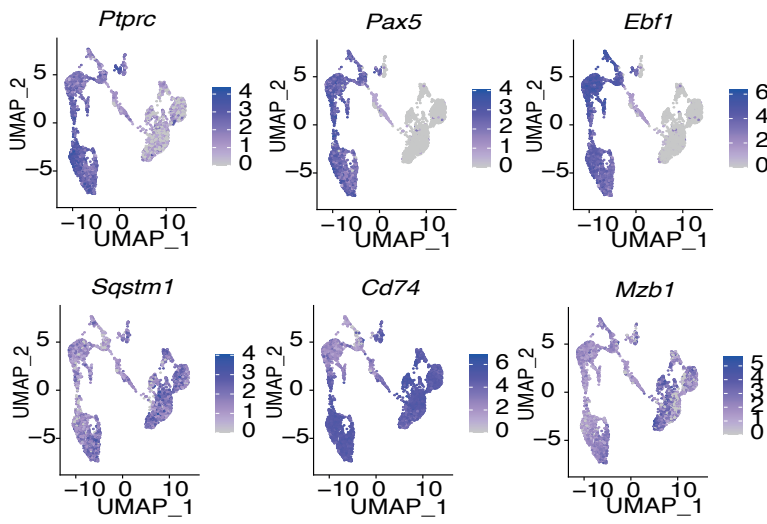


**Suppl. Figure 3**

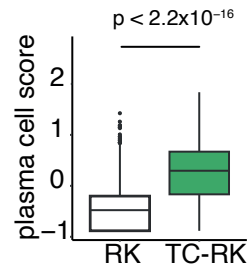


# Suppl. Figure 4

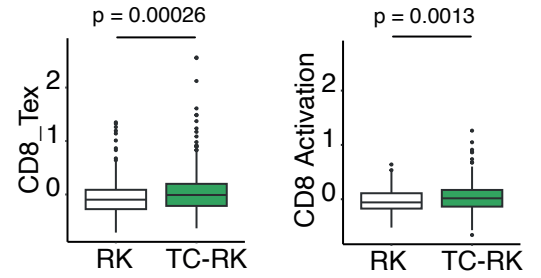
a)



b)



c)



**Suppl. Figure 5**

a)

mouse model	p value	odds ratio
MI <sub>cy1</sub>	1.9x10 <sup>-116</sup>	2.3
Maf-MI <sub>cy1</sub>	8.8x10 <sup>-93</sup>	2.3
BI <sub>cy1</sub>	2.9x10 <sup>-129</sup>	3.0
Kras-BI <sub>cy1</sub>	1.8x10 <sup>-246</sup>	3.7
Trp53-BI <sub>cy1</sub>	9.1x10 <sup>-182</sup>	2.6
CyclinD1-BI <sub>cy1</sub>	1.2x10 <sup>-98</sup>	2.1
Mmset-BI <sub>cy1</sub>	1x10 <sup>-158</sup>	2.6
Maf-BI <sub>cy1</sub>	1.4x10 <sup>-153</sup>	3.0

b)

MM patient ID	infiltration [%]	RANK <sup>+</sup> myeloma cells	intensity
11/18127	40-50	>90	moderate
15/15411	40-50	10	weak
16/1995	50-60	>90	weak
16/11789	70	>90	moderate
20/8767	70	>90	moderate
16/19408	95	30	weak
16/18518	60-70	3	weak
20/13015	95	40	weak
21/2084	40	60	weak
21/15274	40	30	weak